# Estimation of Fractures Orientation from qP reflectivity using Multiazimuthal AVO Analysis

*E.N.S. Gomes, J.C. Costa, J. dos S. Protázio, and I.A. Simões Filho*

**email:** *ellensg@ufpa.br*
**keywords:** *Anisotropy, Fractures orientation, AVO/AVD*

## ABSTRACT

*We investigate the estimation of fractures orientation, strike and dip, through multiazimuthal AVO analysis of $qP$ and its converted waves $qS_1$ and $qS_2$. We assume weak impedance contrast, weak anisotropy and that the fractured medium behaves as an effective transversally isotropic (TI) medium. Under these assumptions, the estimation of fractures orientation is reduced to the estimation of the orientation of an axis of symmetry from $qP$ reflectivity data. Linearized approximations of $qP$ reflectivity are used for inversion.*

## INTRODUCTION

Most hydrocarbon reservoirs occur in fractured formations. In this case, fractures mainly control the reservoir permeability. Since wave propagation in fractured media might be modelled through an effective anisotropic medium (Hudson (1982); Schoenberg and Sayers (1995)), the characterization of the reservoir elastic anisotropy from seismic data may help optimizing oil recovery. Previous works report fractures characterization from AVO/AVD data. Rüger and Tsvankin (1997) show how to estimate vertical fractures strike and fluid content information from $qP$ reflection coefficients data. Perez et al. (1999) use shear wave splitting and P wave reflection data to determine the strike of a vertical set of fractures. Beretta and Drufuca (2002) use diffraction tomography to estimate the fractures density also for vertically fractured medium. We formulate the problem of fractures characterization using the reflections coefficients of a $qP$ incident wave, including converted waves.

## FORWARD PROBLEM

Consider weak impedance contrast and weak anisotropic media separated by a plane interface, $x_3 = 0$.The incident and reflected waves propagate at the upper medium and the transmitted waves propagate through the lower medium. The linearized $qP$ reflectivity across an interface was presented by Gomes et al. (2001). The two anisotropic media are considered as small perturbations around an isotropic homogeneous background. The linear approximations are:

$$
\begin{aligned}
R_{qPqP} \;=\;& \frac{1}{2\;\rho^\circ\,\alpha^2}\Big\{\Big[\Delta C_{11}\cos^4\varphi+\Delta C_{22}\sin^4\varphi+2\,\Delta\,(C_{12}+2C_{66})\cos^2\varphi\sin^2\varphi+\\
& 4\,\Delta C_{16}\,\cos^3\varphi\sin\varphi+4\,\Delta C_{26}\,\cos\varphi\sin^3\varphi\Big]\tan^2\theta\sin^2\theta+2\,\Big[\Delta(C_{13}+2C_{55})\\
& \cos^2\varphi+\Delta(C_{23}+2C_{44})\sin^2\varphi+\Delta(C_{36}+2C_{45})\sin 2\varphi-4\,\Big(\Delta C_{55}\cos^2\varphi+\\
& \Delta C_{44}\sin^2\varphi+\Delta C_{45}\sin 2\varphi\Big)\Big]\sin^2\theta+\Delta C_{33}\cos^2\theta\Big\}+\Big(1-\frac{1}{2\cos^2\theta}\Big)\frac{\Delta\rho}{\rho^\circ}\;;
\end{aligned}
\tag{1}
$$

$$
\begin{aligned}
R_{qS_1qP} \;=\;& \frac{1}{2\,\rho^\circ\,\alpha^2\,\eta(\theta)}\Big\{2\Big[\Delta C_{11}\cos^4\varphi+\Delta C_{22}\sin^4\varphi+2\Delta(C_{12}+2C_{66})\cos^2\varphi\sin^2\varphi+4\\
& \Delta C_{16}\cos^3\varphi\sin\varphi+4\Delta C_{26}\cos\varphi\sin^3\varphi\Big]\sin^3\theta+2\Big[\Delta(C_{13}+2C_{55})\cos^2\varphi+\\
& \Delta(C_{23}+2C_{44})\sin^2\varphi+2\Delta(C_{36}+2C_{45})\sin 2\varphi-4\Big(\Delta C_{55}\cos^2\varphi+\Delta C_{44}\sin^2\varphi+\\
& \Delta C_{45}\sin 2\varphi\Big)\Big]\sin\theta\cos\,2\,\theta-\Delta C_{33}\sin\,2\,\theta\cos\theta+\frac{1}{\kappa\,K(\theta)}\Big\{\,2\,\Big[\,\Delta C_{14}\cos^2\varphi\,\sin\varphi+\\
& \Delta C_{15}\cos^3\varphi+\Delta C_{24}\sin^3\varphi+\Delta C_{25}\cos\varphi\sin^2\varphi+\Delta C_{46}\sin\varphi\,\sin 2\varphi+\Delta C_{56}\cos\varphi\\
& \sin 2\varphi\Big]\sin^2\theta\,\left(2\kappa\,\omega(\theta)-1\right)+2\Big[\Delta C_{35}\cos\varphi+\Delta C_{34}\sin\varphi\Big]\cos\theta\,\left(\cos\theta-2K(\theta)\,\omega(\theta)\right)+\\
& 2\Big[\Delta C_{55}\cos^2\varphi+\Delta C_{44}\sin^2\varphi+\Delta C_{45}\sin 2\varphi\Big]\sin 2\theta\Big(\kappa^2\sin^2\theta-K^2(\theta)\Big)\Big\}\Big\}-\\
& \Big(\frac{\sin\theta}{K(\theta)}\Big)\frac{\Delta\rho}{\rho^\circ}\;;
\end{aligned}
\tag{2}
$$

$$
\begin{aligned}
R_{qS_2qP} \;=\;& \frac{1}{\rho^\circ\,\alpha^2K(\theta)}\Big\{\frac{1}{\kappa}\Big\{\Big[\Delta C_{14}\cos^3\varphi-\Delta C_{25}\sin^3\varphi+\Big(\Delta C_{24}\sin\varphi-\Delta C_{15}\cos\varphi\Big)\cos\varphi\\
& \sin\varphi+\Big(\Delta C_{46}\cos\varphi-\Delta C_{56}\sin\varphi\Big)\sin 2\,\varphi\Big]\sin^2\theta\;+\;\Big[\Delta C_{45}\cos 2\,\varphi+\Delta C_{44}\cos\varphi\\
& \sin\varphi-\Delta C_{55}\,\cos\varphi\,\sin\varphi\Big]\sin 2\,\theta+\Big[\Delta C_{34}\cos\varphi-\Delta C_{35}\sin\varphi\Big]\cos^2\theta\Big\}-\frac{1}{\eta(\theta)}\\
& \Big\{\Big[\Delta C_{16}\cos^2\varphi\,(\,\cos^2\varphi-3\,\sin^2\varphi\,)+\Delta C_{26}\sin^2\varphi\,(\,3\,\cos^2\varphi-\sin^2\varphi\,)+\Big(\Delta C_{22}\\
& \sin^2\varphi-\Delta C_{11}\cos^2\varphi\Big)\cos\varphi\sin\varphi+\Delta(C_{12}+2C_{66})\cos\varphi\sin\varphi\cos 2\varphi\Big]\sin^3\theta+\\
& \Big[\Delta C_{14}\cos\varphi\big(\cos^2\varphi-2\,\sin^2\varphi\big)+3\,\Big(\Delta C_{24}\sin\varphi-\Delta C_{15}\cos\varphi\Big)\sin\varphi\,\cos\varphi+\\
& 2\,\Delta C_{46}\sin\varphi\big(2\,\cos^2\varphi-\sin^2\varphi\big)+\Delta C_{25}\,\sin\varphi\big(2\,\cos^2\varphi-\sin^2\varphi\big)+2\,\Delta C_{56}\cos\varphi\\
& \big(\cos^2\varphi-2\,\sin^2\varphi\big)\Big]\cos\theta\sin^2\theta+\Big[\Delta(C_{36}+2C_{45})\cos 2\varphi-\Delta(C_{13}+2C_{55})\sin\varphi\\
& \cos\varphi+\Delta(C_{23}+2C_{44})\sin\varphi\cos\varphi\Big]\cos^2\theta\sin\theta+\Big[\Delta C_{34}\cos\varphi-\Delta C_{35}\sin\varphi\Big]\cos^3\theta\Big\}\Big\}.
\end{aligned}
\tag{3}
$$

Where $\theta$ is the incidence angle; $\varphi$ is the azimuth angle; $\kappa = \alpha\,/\,\beta$ is the ratio between S-wave and P-wave velocities in the isotropic reference medium; $\rho^\circ$ is the background density; $\Delta\rho$ is the average density contrast across the interface; $K(\theta) = \sqrt{1-\kappa^2\sin^2\theta}$, $\omega(\theta) = \kappa\sin^2\theta + K(\theta)\cos\theta$ and $\eta(\theta) =$

$\kappa \cos\theta + K(\theta)$; $\Delta C_{ij}$ is the average elastic constants contrast across the two media defined for

$$\Delta C_{ij} = \frac{C_{ij}^{(T)} - C_{ij}^{(I)}}{2}. \tag{4}$$

Where $C_{ij}^{(T)}$ indicates the transmission medium elastic tensor and $C_{ij}^{(I)}$ is the elastic tensor in the medium of incidence, $i, j = 1, ..., 6,$ in the standard reduced notation(Helbig (1994)). The equations (1) was presented previously by Vavrycuk and Psencik (1998) and the equations (2) and (3) where also derived in Jílek (2002) in a somewhat different form. In order to derive the expression above, the polarization directions in the background media were chosen to be the SV and SH direction, which makes them more suitable when the medium of incidence has azimuthal symmetry. However, if degenerate perturbations theory can be used to compute more suitable polarization directions for shear waves(Jech and Psencik (1989)).

## INVERSION PROBLEM

Using the equation (1) - (3) the inversion problem is reduced to the solution of a linear system:

$$\mathbf{r} = \mathbf{A}(\mathbf{C}^0, \varphi, \theta)\mathbf{p} \tag{5}$$

Where $\mathbf{r}$ is the vector containing the observations ($R_{qPqP}$, $R_{qS_1qP}$, $R_{qS_2qP}$), $\mathbf{p}$ is the vector containing the density and elastic parameters contrasts and the matrix $\mathbf{A}(\mathbf{C}^0, \varphi, \theta)$ depends only on the background medium and the directions of the incident $qP$ wave.Based on SVD analysis of $\mathbf{A}$, multiazimuthal data is required to produce stable estimates . 3-D VSP experiments (Leaney et al. (1999)) might provide this kind of data. The vector $\mathbf{p}$ is organized as bellow:

$$\begin{pmatrix} \mathrm{p}_1 = \Delta C_{11} & \mathrm{p}_2 = \Delta(C_{12} + 2C_{66}) & \mathrm{p}_3 = \Delta(C_{13} + 2C_{55}) \\ \mathrm{p}_4 = \Delta C_{22} & \mathrm{p}_5 = \Delta(C_{23} + 2C_{44}) & \mathrm{p}_6 = \Delta C_{33} \\ \mathrm{p}_7 = \Delta C_{44} & \mathrm{p}_8 = \Delta C_{55} & \mathrm{p}_9 = \Delta C_{14} \\ \mathrm{p}_{10} = \Delta C_{15} & p_{11} = \Delta C_{16} & \mathrm{p}_{12} = \Delta C_{24} \\ \mathrm{p}_{13} = \Delta C_{25} & \mathrm{p}_{14} = \Delta C_{26} & \mathrm{p}_{15} = \Delta C_{34} \\ \mathrm{p}_{16} = \Delta C_{35} & \mathrm{p}_{17} = \Delta C_{36} & \mathrm{p}_{18} = \Delta C_{45} \\ \mathrm{p}_{19} = \Delta C_{46} & \mathrm{p}_{20} = \Delta C_{56} & \mathrm{p}_{21} = \Delta\rho/\rho^\circ \end{pmatrix} \tag{6}$$

For estimate of the parameters $\mathbf{p}$ we assume:

- weak impedance contrast, weak anisotropy;
- the medium of incidence is isotropic and coincides with the background media used for linearization.

For the estimation of fractures orientation we assume that the fractured medium behaves as an effective TI medium with its axis of symmetry perpendicular to the plane of fractures.
Under these assumptions, our goal is to estimate the orientation of the symmetry axis from the elastic parameters estimated from inversion. If the axis of symmetry is not aligned with one of the coordinate axis the plane of symmetry containing the axis forms an angle $\Psi$ with the $x_3$ (Figure 1). This angle can be determined from the relation:

$$\tan 2\Psi = \frac{2\left(C_{16} + C_{26}\right)}{\left(C_{22} - C_{11}\right)} \tag{7}$$

Unfortunately two angles have the same tangent $\Psi$ and $\Psi + \pi/2$. Rotating the elastic parameters estimated by the negative of one of these angles aligns the symmetry plane containing the tilted axis along the $x_1$ or $x_2$ axis. We can always choose the rotation, which align the symmetry plane containing the tilted axis along the $x_1$ axis and use the expression below to determine the dip angle $\Theta$

$$\tan 2\Theta = \frac{2\left(C_{15} + C_{35}\right)}{\left(C_{11} - C_{33}\right)} \tag{8}$$

Under our assumptions, dip angle can be estimated from the inversion results except by the same ambiguity as before, i.e.,$\Theta$ or $\Theta+\pi/2$. This ambiguity can be resolved rotating the parameter by the negative of these values and observing the differences $C_{11}-C_{22}$ and $C_{33}-C_{22}$ . If the first difference is zero the axis of symmetry is aligned along $x_3$ and the dip angle is $\Theta+\pi/2$ otherwise $C_{33}-C_{22}$ is zero and the axis is aligned along $x_1$ and the dip angle is $\Theta$. It is always possible to perform this rotation, all the combination of elastic parameters required to perform this rotation are estimated from inversion. If the axis of symmetry coincides with one of the coordinate axis the algorithm fails. In this case orientation can be determined using the alternatives:

$$\begin{array}{ll} a) & \text{If } C_{22}=C_{33} \text{ and } C_{44}\neq C_{55} \text{ the axis is along } x_1. \\ b) & \text{If } C_{11}=C_{33} \text{ and } C_{44}\neq C_{55} \text{ the axis is along } x_2. \\ c) & \text{If } C_{11}=C_{22} \text{ and } C_{44}=C_{55} \text{ the axis is along } x_3. \end{array} \tag{9}$$

The resolution and stability of the inversion was evaluated using SVD analysis and numerical simulations. For the simulations several synthetic data sets were computed using the exact expressions for the reflection coefficients. Each synthetic data set was contaminated by Gaussian noise using 100 random seeds to initialize the random number generator. These data were inverted and the mean and standard deviations of the parameters used to evaluate stability.

## EXAMPLES

The elastic parameters and the orientation the axis symmetry was estimated the of inversion from (1), (2) and (3) joins for two models. The synthetic data set was generated solving the Zoeppritz equations (Gomes (1999)). The azimuth range is from $0^\circ$ to $360^\circ$ with $15^\circ$ intervals and the incidence angle varies from $0^\circ$ to $30^\circ$ with $1^\circ$ intervals. This data set was contaminated with different level Gaussian random noise of amplitude of $5\%$ to $20\%$ of the mean absolute value of the observations. The 100 data sets, each with a different noise contamination, were inverted. Both models have weak contrast $\Delta\rho/\rho^\circ, \Delta\alpha/\alpha, \Delta\beta/\beta$ are smaller than $10\%$ and weak anisotropy.
In the first model the top medium is an isotropic $\rho = 2.65$g/cm$^3$ $\alpha = 4.00$ km/s e $\beta = 2.31$km/s. The bottom medium is TI with horizontal axis and its density is $\rho = 2.5g/$cm$^3$ and its elastic tensor is:

$$C_{ij} = \begin{bmatrix} 31.10 & 10.37 & 10.37 & 0.00 & 0.00 & 0.00 \\ & 40.43 & 12.69 & 0.00 & 0.00 & 0.00 \\ & & 40.43 & 0.00 & 0.00 & 0.00 \\ & & & 13.86 & 0.00 & 0.00 \\ & & & & 12.38 & 0.00 \\ & & & & & 12.38 \end{bmatrix} \tag{10}$$

Table 1 presents the average and standard deviations of the numerical simulation results,

| (**p**) | Extac | Mean | Error | $C_{ij}$ | Exact | Mean | Error |
|---|---|---|---|---|---|---|---|
| $\Delta C_{11}$ | -0.0682 | -0.0632 | $1.75\%$ | $C_{11}$ | 31.10 | 31.93 | $0.65\%$ |
| $\Delta(C_{12}+2C_{66})$ | -0.0439 | -0.0423 | $4.38\%$ | $C_{12}+2C_{66}$ | 35.13 | 35.60 | $0.5\%$ |
| $\Delta(C_{13}+2C_{55})$ | -0.0439 | -0.04261 | $1.17\%$ | $C_{13}+2C_{55}$ | 35.13 | 34.55 | $0.74\%$ |
| $\Delta C_{22}$ | -0.0119 | -0.0095 | $14.23\%$ | $C_{22}$ | 40.43 | 40.73 | $0.54\%$ |
| $\Delta(C_{23}+2C_{44})$ | -0.0120 | -0.0121 | $3.59\%$ | $C_{23}+2C_{44}$ | 40.41 | 39.71 | $0.65\%$ |
| $\Delta C_{33}$ | -0.0119 | -0.01273 | $1.57\%$ | $C_{33}$ | 40.43 | 39.90 | $0.07\%$ |
| $\Delta C_{44}$ | -0.0017 | -0.0017 | $3.39\%$ | $C_{44}$ | 13.86 | 13.69 | $0.35\%$ |
| $\Delta C_{55}$ | -0.0107 | -0.0107 | $1.35\%$ | $C_{55}$ | 12.38 | 12.17 | $0.39\%$ |
| $\Delta\rho/\rho^\circ$ | -0.01 | -0.008 | $4.9\%$ | $\rho$ | 2.60 | 2.61 | $0.079\%$ |

**Table 1:** Numerical simulation results. Exact value, mean and the relative error of the estimated values for $\mathrm{p}_1-\mathrm{p}_8$, $\mathrm{p}_{21}$ and elastic parameters (in GPa) in the transmitted medium. The data noise level is $10\%$ of the observations maximum value.

The parameters $\Delta C_{11},\ \Delta(C_{12}+2C_{66}),\ \Delta(C_{13}+2C_{55}),\ \Delta C_{22}, \Delta(C_{23}+2C_{44}), \Delta C_{33}, \Delta C_{44}, \Delta C_{55}$ and $\Delta\rho/\rho^\circ$ presented a relative error lower then $15\%$ which characterizes a stable estimation. The remain-

ing parameters, $p_9 - p_{20}$, have very small mean ($10^{-4}$) and the relative error cannot be computed. These results holds for data noise level lower than $20\%$. We must use (9) in order to estimate the orientation of the symmetry axis. The difference between $C_{22}$ and $C_{33}$ is smaller than the difference between these parameter and $C_{11}$. Noticing also the difference between $C_{44}$ and $C_{55}$, we conclude the medium is TI with horizontal axis.The results are the same for $20\%$ noise level.
In the second model the top medium is isotropic $\rho = 2.60$ gcm$^3$, $\alpha = 4.600$ km/s and $\beta = 2.810$ km/s. The bottom medium is a sandstone, its elastic tensor is TI with vertical axis and its Thomsen parameters (Thomsen (1986)) are $\rho = 2.50$ g/cm$^3$, $\alpha = 4.476$ km/s and $\beta = 2.841$ km/s, $\varepsilon = 0.097$, $\delta = 0.091$, $\gamma = 0.051$. This medium was rotated of $60°$ anticlockwise around $x_3$ axis and after that rotated of $30°$ anticlockwise around the new $x_2$ axis (see Figure 1).

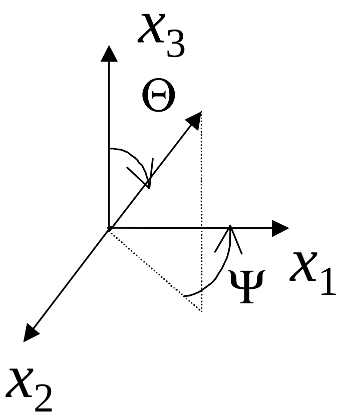


**Figure 1:** Coordinate axis. The angle $\Psi$ is the azimuthal and the angle $\Theta$ is the incidence.

The Figures 2(a), 3(a), 4(a) present the stereogram of the exact synthetic data for each wave type. Figures 2(b), 3(b), 4(b) present the corresponding stereogram computed from the mean of the parameters estimated from 100 numerical simulations.

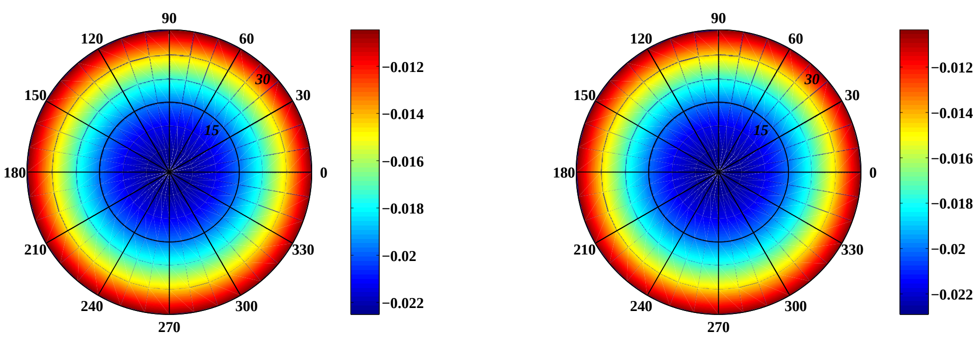


**(a)** Exact $R_{qPqP}$.

**(b)** $R_{qPqP}$ of the inverted model.

**Figure 2:** Stereogram for the $R_{qPqP}$

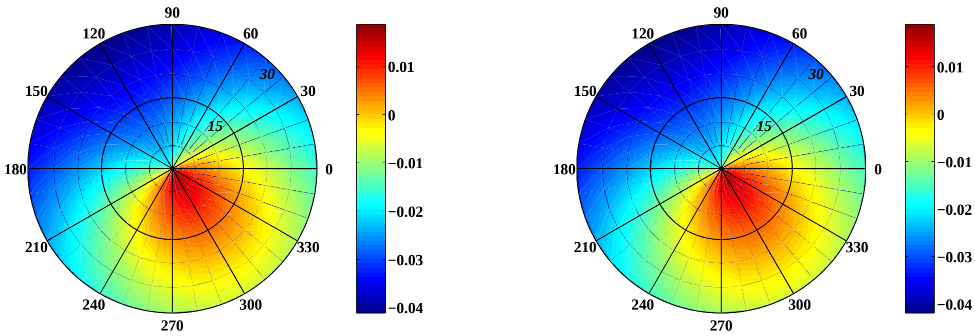


**(a)** Exact $R_{qS_1qP}$. **(b)** $R_{qS_1qP}$ of the inverted model.

**Figure 3:** Stereogram for the $R_{qS_1qP}$

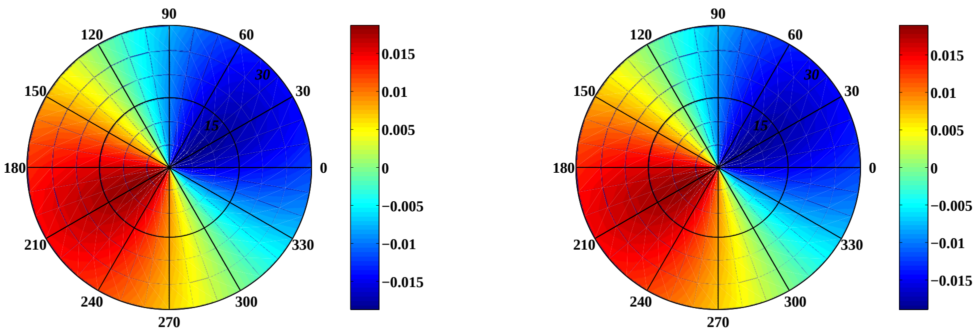


**(a)** Exact $R_{qS_2qP}$. **(b)** $R_{qS_2qP}$ of the inverted model.

**Figure 4:** Stereogram for the $R_{qS_2qP}$

The symmetry of the $R_{PP}$ stereogram indicates its insensitivity to the dip of fractures. However, the SVD shows that $R_{qPqP}$ data is required to estimate the fractures dip. The estimated models fit the data with maximum residual of the order of $10^{-3}$ for every data set. The results of the numerical simulations for this model for $10\%$ noise level are presented in Table 2 which shows for the exact value of the **p**, its the average of the estimated, the ratio of the of the standard deviations. The results of the numerical simulations for this model for several noise levels are presented in Table 3 the of the average of the estimates of the symmetry axis azimuth and dip and the ratio of the standard deviation of the estimation over their average value.

| Param (**p**) | Extac Value | Mean | Error |
|---|---|---|---|
| $\Delta C_{11}$ | 0.019 | 0.021 | $9.42\%$ |
| $\Delta(C_{12}+2C_{66})$ | 0.016 | 0.017 | $11.22\%$ |
| $\Delta(C_{13}+2C_{55})$ | 0.002 | 0.003 | $32.49\%$ |
| $\Delta C_{22}$ | 0.013 | 0.013 | $13.63\%$ |
| $\Delta(C_{23}+2C_{44})$ | 0.001 | 0.001 | $88.11\%$ |
| $\Delta C_{33}$ | -0.013 | -0.013 | $2.26\%$ |
| $\Delta C_{44}$ | -0.002 | -0.002 | $10.85\%$ |
| $\Delta C_{55}$ | -0.001 | -0.001 | $18.76\%$ |
| $\Delta C_{14}$ | -0.002 | -0.002 | $49.74\%$ |
| $\Delta C_{15}$ | 0.005 | 0.005 | $37.23\%$ |
| $\Delta C_{16}$ | 0.003 | 0.003 | $23.48\%$ |
| $\Delta C_{24}$ | -0.009 | -0.008 | $19.66\%$ |
| $\Delta C_{25}$ | 0.001 | 0.001 | $77.69\%$ |
| $\Delta C_{26}$ | 0.003 | 0.003 | $26.72\%$ |
| $\Delta C_{34}$ | -0.008 | -0.008 | $0.38\%$ |
| $\Delta C_{35}$ | 0.005 | 0.005 | $0.65\%$ |
| $\Delta C_{36}$ | 0.0003 | 0.001 | $81.68\%$ |
| $\Delta C_{45}$ | 0.0006 | 0.0007 | $21.46\%$ |
| $\Delta C_{46}$ | 0.002 | 0.002 | $50.86\%$ |
| $\Delta C_{56}$ | -0.003 | -0.003 | $30.85\%$ |
| $\Delta\rho/\rho^{\circ}$ | -0.02 | -0.02 | $2.55\%$ |

**Table 2:** Numerical simulation results. Exact value, estimated mean value and relative error of the parameters . The data noise level is $10\%$ of the observations maximum value.

| Noise Level | Fract. Azimuth (Exact $\Psi = 60°$) | Deviation | Fract. Dip (Exact $\Theta = 30°$) | Deviation |
|---|---|---|---|---|
| $5\%$ | $60.05°$ | $\pm 2.51°$ | $29.43°$ | $\pm 1°$ |
| $10\%$ | $60.79°$ | $\pm 5.38°$ | $29.31°$ | $\pm 1.42°$ |
| $20\%$ | $58.89°$ | $\pm 10°$ | $28.48°$ | $\pm 7.35°$ |

**Table 3:** Numerical simulation results for different noise levels. The ratio of the standard deviation of the estimates over the mean value is also presented to indicate the stability.

The SVD analysis and the relative error of the estimated parameters in numerical simulations show that, although parameters $\Delta C_{14}$, $\Delta C_{15}$, $\Delta C_{16}$, $\Delta C_{24}$, $\Delta C_{25}$, $\Delta C_{26}$, $\Delta C_{36}$, $\Delta C_{45}$, $\Delta C_{46}$, $\Delta C_{56}$ present instability, the estimates of the symmetry axis orientation is stable. Since the recovery of the orientation depends on nonlinear functions of the parameters SVD analysis can not be applied to determine stability.

## CONCLUSIONS

Several tests were performed with models with weak impedance contrast and weak anisotropy and also with models that violated some of these assumptions. Also different azimuth rages and incidence angles were used. From these test we drew the following:

1. $R_{qPqP}$, $R_{qS_1qP}$ and $R_{qS_2qP}$ are required to recover the orientation from multiazimuthal AVO data only.
2. The minimum azimuth interval to recover stable estimates of orientations is $\varphi = 30°$
3. The minimum incidence angle range is $\theta = 30°$.
4. Though the estimates of elastic parameters contrasts vary during the simulations, the estimates of the orientation angles are reliable for moderate noise levels $(< 10\%)$.

5. The estimates of fractures strike is more sensitive to noise than the fractures dip.
6. The estimates are accurate only for models with weak impedance contrast and weak anisotropy.

We presented an algorithm to estimate fractures orientation using multiazimuthal AVO analysis. Reflection coefficients of $R_{qPqP}$, $R_{qS_1qP}$ and $R_{qS_2qP}$ are needed to determine the fractures dip . Though the assumption of an effective TI behavior for fractures is restrictive, its validity can be checked from the symmetries of the elastic tensor derived from the inverted parameters . For a weak TI medium and weak impedance contrast, the estimates of fractures orientation are unique and stable for moderate noise levels.

## ACKNOWLEDGMENTS

The authors acknowledge the financial support of the Project FINEP/CTPETRO/UFPA.

## REFERENCES

Beretta, M. M. Bernasconi, G. and Drufuca, G. (2002). AVO and AVA inversion of fractured reservoir characterization. *Geophysics*, 67(1):300–306.

Gomes, E. N. S. (1999). Reflectivity of P waves in anisotropic media. Master's thesis, Department of Mathematics of Universidade Federal do Pará. (in Portuguese).

Gomes, E. N. S., Protázio, J., Costa, J., and Simões-Filho, I. (2001). Linearization of qP wave reflection coefficients in anisotropic media. *Brazilian Journal of Geophysics*, 19:48–60. (in Portuguese).

Helbig, K. (1994). *Foundations of Anisotropy for Exploration Seismics*, volume 22 of *Handbook of Geophysical Exploration*. Pregamon, Oxford.

Hudson, J. A. (1982). Wave speeds and attenuation of elastic waves in material containing cracks. *Geophys. J. R. astr Soc*, 64:133–150.

Jech, J. and Psencik, I. (1989). First-order perturbation method for anisotropic media. *Geophys. J. Int.*, 99:369–376.

Jílek, P. (2002). Converted PS-wave reflection coefficients in weakly anisotropic media. *Pure and Applied Geophysics*, 7-8:1527–1562.

Leaney, W. S., Sayers, C. M., and Miller, D. E. (1999). Analysis of multiazimuthal VSP data for anisotropy and AVO. *Geophysics*, 64(4):1172–1180.

Perez, M. A., Gibson, R. L., and Toksoz, N. (1999). Detection of fracture orientation using azimuthal variation of P-wave AVO responses. *Geophysics*, 64:1253–1265.

Rüger, A. and Tsvankin, I. (1997). Using avo for fracture detection: Analytic basis and practical solutions. *The Lead Edge*, 16(10):1429–1434.

Schoenberg, M. and Sayers, C. (1995). Seismic anisotropy of fractures. *Geophysics*, 60:204–211.

Thomsen, L. (1986). Weak elastic anisotropy. *Geophysics*, 51(10):1954–1966.

Vavrycuk, V. and Psencik, V. (1998). PP-wave reflection coefficients in weakly anisotropic elastic media. *Geophysics*, 63(6):2129–2141.